Absorption-Based Ranging from Ambient Thermal Radiation without Known Emissivities

Unay Dorken Gallastegi[1], Hoover Rueda-Chacon[1], Martin J. Stevens[2], and Vivek K Goyal[1]

[1]*Boston University, Boston, MA, USA*
[2]*National Institute of Standards and Technology, Boulder, CO, USA*
udorken@bu.edu, rueda@bu.edu, marty@nist.gov, v.goyal@ieee.org

Abstract: We present passive absorption-based ranging using long-wave infrared hyperspectral measurements of an outdoor scene. Regularization and parametric modeling of transmittance enable good accuracy without knowing temperatures or emissivities of scene objects, as validated with lidar.

Introduction. Conventional depth estimation techniques in autonomous navigation use time-of-flight or stereo image pairs to infer depth. Ranging techniques such as lidar have been extensively studied [1]; however, when stealthiness is important, active ranging methods are limited to nearby objects and passive methods are preferred. In passive ranging, stereo-based techniques are commonly used. These require pixel matching between the camera pair, which may be problematic for low-textured scenes. Although not typically used, spectrally resolved measurements at atmospheric absorption bands provide depth cues that can be exploited for ranging [2]. Compared to conventional depth estimation techniques, absorption-based ranging is stealthy and does not rely on scene texture, thus making it an alternative for challenging navigation conditions.

Although mostly transparent, the long-wave infrared (LWIR) window (8-14 μm) provides information about depth, mainly due to water vapor absorption, and intrinsic object properties. Compared to other spectral bands, most of the ambient black-body radiation is concentrated in the LWIR band. In remote sensing applications, atmospheric absorption effects are typically removed from the measurements by atmospheric correction techniques, extracting information about intrinsic object properties such as temperature and emissivity profile [3]. In contrast to such techniques, we exploit the atmospheric absorption in the measurements to estimate depth.

Method and Results. An object with emissivity profile $\varepsilon(\lambda)$ and temperature T emits light with radiance $\varepsilon(\lambda)B(\lambda;T)$, where $B(\lambda;T)$ is the ideal black-body spectrum. The emitted light is attenuated by the atmospheric transmittance function $\tau(\lambda;d) = 10^{-\alpha(\lambda)d}$, where $\alpha(\lambda)$ represents the atmospheric attenuation (dB/m) upon travelling through d meters of air, resulting in $\tau(\lambda;d)\varepsilon(\lambda)B(\lambda;T)$. Air at temperature T_{air} also emits light while absorbing it, contributing $(1-\tau(d;\lambda))B(\lambda;T_{air})$ to the measurement. Thus, the light arriving at the sensor can be modeled as

$$L_S(\lambda) = \tau(\lambda;d)\varepsilon(\lambda)B(\lambda;T) + (1-\tau(\lambda;d))B(\lambda;T_{air}). \tag{1}$$

We assume that T_{air} and the atmospheric parameters to calculate the attenuation profile are known. For a K-long spectrally resolved measurement, the inversion of Eq. (1) is ill-conditioned; it has $K+2$ unknowns, including T, d and K-dimensional ε.

Following the ideas proposed in [4], we formulate the inversion as a minimization problem on a group of pixels that correspond to a single object (same emissivity and distance) with varying temperature per pixel. We use an emissivity-smoothing regularizer, exploiting the fact that emissivity profiles of solid objects are smooth compared to the sharp transitions in the attenuation profile. The function we minimize is

$$L(d,T,\varepsilon) = \sum_{i=1}^{N}\sum_{k=1}^{K}(\hat{y}_{i,k}(d,T,\varepsilon) - y_{i,k})^2 + \rho\sum_{k=1}^{K-1}(\varepsilon_{k+1}-\varepsilon_k)^2, \tag{2}$$

where $i \in \{1,\dots,N\}$ is the pixel index inside the group, $k \in \{1,\dots,K\}$ is the wavelength index, $y_{i,k}$ is the measurement at pixel i and wavelength k, $\hat{y}$ is the light generated by the parameterized forward model following (1), and ρ is a parameter that controls the extent of the smoothing regularizer. We use gradient descent to minimize the function $L(d,T,\varepsilon)$. The optimization is completed separately on disjoint 5×5 pixel patches that tile the field of view of the hyperspectral camera.

Figure 1 shows the results of our method performed on an LWIR hyperspectral image acquired just after sunset for a scene with rolling, grassy terrain with a small grove of trees in the foreground and a forest in the background.

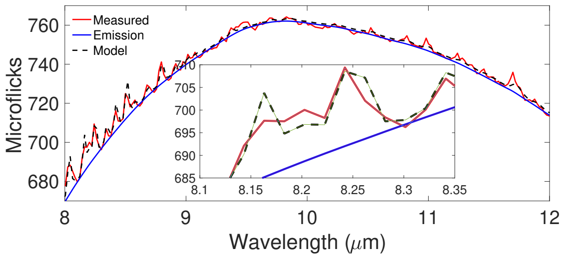

(a) Measurement of a grass pixel at around 100 m

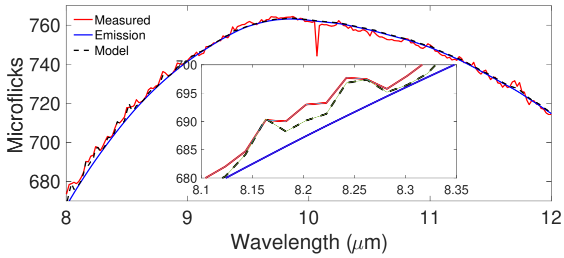

(b) Measurement of a grass pixel at around 8 m

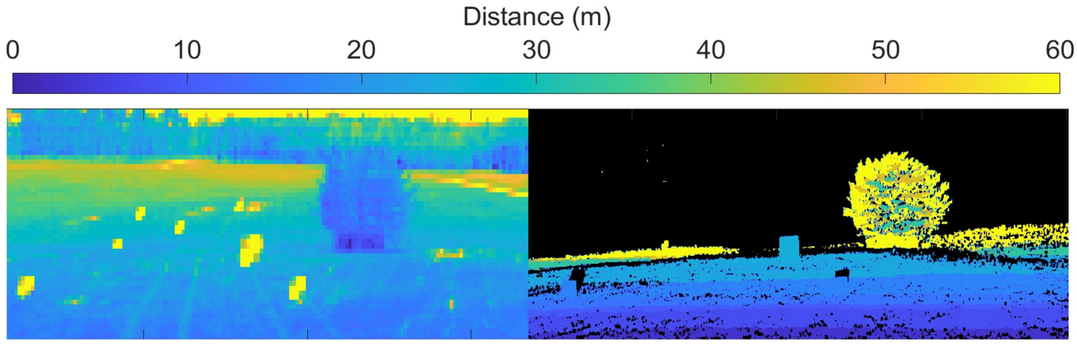

(c) Estimated depth map (left) and reference depth map from high-resolution lidar sensor (right).

Fig. 1: Results of our algorithm on a LWIR hyperspectral image. (a) and (b) show the measurements and the fit at the convergence points for a far grass and near grass pixel, respectively. The solid red lines correspond to the measurement, the solid blue lines represent the estimated object emission ($\varepsilon(\lambda)B(\lambda,T)$), and the dashed black lines represent the forward model with the estimated parameters. In (c) we show the absorption-based estimated depth map on the left and the depth map measured with a high-resolution lidar system on the right. Black represents missing lidar data.

Figures 1a and 1b show two measurements from pixels containing far and near grassy areas. The intrinsic parameters of these objects are very similar to each other, as can be verified from the blue solid lines. The differences between the measurements are mostly due to distance. If we concentrate on the 8–9 μm range, the far measurement contains more atmospheric effects as it travels a longer distance through air. Comparing the estimated depth map in Fig. 1c with the lidar map, our method is quite successful at capturing the gradient in distance from foreground to background for the grassy terrain. The method fails for the calibration targets (bright yellow spots) and the background forest. The target distances are overestimated due to reflected sky light, which is not accounted for in our current model. The forest distance is underestimated, possibly because of variations in air temperature, which our model assumes is constant over the whole scene. In the near future, which we hope to address these problems by separating the reflected light from the emitted light in the forward modeling and by conducting per-pixel air temperature estimation from mid-wave infrared (MWIR) spectra, where atmospheric attenuation is stronger.

Given the low contrast in the grassy regions of the image, we believe this is a difficult scenario for a stereo-matching algorithm to succeed. We emphasize that no prior information about the objects' temperatures or emissivity spectra was assumed, except for smoothness of the emissivity profiles.

Acknowledgments. This work was supported in part by the US Defense Advanced Research Projects Agency (DARPA) Invisible Headlights program under contract number HR0011-20-S-0045. Data provided by the U.S. Army Night Vision and Electronic Sensors Directorate and Johns Hopkins University Applied Physics Laboratory.

References

1. J. Rapp, J. Tachella, Y. Altmann, S. McLaughlin, and V. K. Goyal, "Advances in single-photon lidar for autonomous vehicles: Working principles, challenges, and recent advances," IEEE Signal Process. Mag. **37**, 62–71 (2020).
2. H. Yu, B. Liu, Z. Yan, and Y. Zhang, "Passive ranging using a filter-based non-imaging method based on oxygen absorption," Appl. Opt. **56**, 7803–7807 (2017).
3. D. Manolakis, M. Pieper, E. Truslow, R. Lockwood, A. Weisner, J. Jacobson, and T. Cooley, "Longwave infrared hyperspectral imaging: Principles, progress, and challenges," IEEE Geosci. Remote. Sens. Mag. **7**, 72–100 (2019).
4. S. Kim, J. Shin, and S. Kim, "AT^{2}ES: Simultaneous atmospheric transmittance-temperature-emissivity separation using online upper midwave infrared hyperspectral images," Remote. Sens. **13** (2021).